Sensitivity study of the Regional Climate Model RegCM4 to different convective schemes over West Africa

Brahima KONÉ[1], Arona DIEDHIOU[1, 2], N'datchoh Evelyne TOURÉ[1], Mouhamadou Bamba SYLLA[3], Filippo GIORGI [4], Sandrine ANQUETIN[2], Adama BAMBA[1], Adama DIAWARA[1], Arsene Toka KOBEA[1]

[1]LAPAMF, Université Félix Houphouët Boigny, Abidjan, Côte d'Ivoire

[2]Univ. Grenoble Alpes, IRD, CNRS, Grenoble INP, IGE, F-38000 Grenoble, France

[3]WASCAL Centre of Competence, Ouagadougou, Burkina Faso

[4]International Centre for Theoretical Physics (ICTP), Trieste, Italy

Correspondence to: Arona DIEDHIOU (arona.diedhiou@ird.fr)

Abstract. The latest version of RegCM4 with CLM4.5 as land surface scheme was used to assess the performance and the sensitivity of the simulated West African climate system to different convection schemes. The sensitivity studies were performed over the West Africa domain from November 2002 to December 2004, at spatial resolution of 50km x 50km and involved five (5) convective schemes: (i) Emanuel; (ii) Grell; (iii) Emanuel over land and Grell over ocean (Mix1); (iv) Grell over land and Emanuel over ocean (Mix2); and (v) Tiedtke. All simulations were forced with ERA-Interim data. Validation of surface temperature at 2m and precipitation were conducted using respectively data from the Climate Research Unit (CRU), Global Precipitation Climatology Project (GPCP) and Tropical Rainfall Measurement Mission (TRMM) during June to September (rainy season), while the simulated atmospheric dynamic was compared to ERA-Interim data. It is worth noting that the few previous similar sensitivity studies conducted in the region was performed using BATS as land surface scheme and involved less convective schemes. Compared with the previous version of RegCM, RegCM4-CLM also shows a general cold bias over West Africa whatever the convective scheme used. This cold bias is more reduced when using Emanuel convective scheme. In term of precipitation, the dominant feature in model simulations is a dry bias, better reduced when using Emanuel convective scheme. Considering the good performance with respect to a quantitative evaluation of the temperature and precipitation simulations over the entire West Africa domain and its sub-regions, Emanuel convective scheme is recommended for the study of the West African climate system.

1 Introduction

Agriculture over West Africa relies mainly on rainfall and is strongly dependent on the West African monsoon. Therefore, the onset, cessation and the amount of expected precipitation associated with the West African Monsoon are of great importance for farmers and accurate simulation and prediction of rainfall and temperature are crucial for various sectors, such as agriculture, energy and health, and for decision-makers. Rainfall over West Africa is strongly related to the meridional migration of the Inter-Tropical zone of convergence (ITCZ) and is modulated by successive active and inactive phases of the monsoon system (Sultan et al., 2003a; Janicot et al., 2011). After a quasi-stationary position around 5° N between mid-April and end of June, the rainfall maxima present an abrupt shift toward the north to hold another quasi-stationary position around 11°N in July-August, bringing precipitation over Central Sahel region (Sultan and Janicot, 2000). This abrupt northward shift is the monsoon ''onset'' over the Sahel and contrasts with the smooth southward retreat of the ITCZ, followed by the second rainy season over the Guinean Coast in October–November (Sultan et al., 2003b; Janicot et al., 2011). In addition, atmospheric circulations through African Easterly Jet (AEJ), Tropical Easterly Jet (TEJ) and their interaction with convection play an important role in the West African Monsoon (WAM) system (Nicholson 2013) and modulate the summer rainfall (Sylla et al., 2013a). Various climate modeling tools have been applied over West Africa for studying and better understanding of the WAM.

General circulation models (GCMs) are unable to include the effects of regional features (Xue et al., 2010) due to their relatively coarse resolution. Regional Climate Models (RCMs) are relevant tools for this purpose since they allow land surface heterogeneity and fine-scale forcing such as complex topography and vegetation variations (Paeth and al., 2006). Moreover, previous studies have shown that they are able to reasonably simulate the WAM climatology (Kamga and Buscarlet, 2006; Sylla et al., 2009) and its variability (Diallo et al., 2012). RCMs contributed to improve our knowledge of the interactions between atmospheric and surface factors affecting the precipitation (Sylla et al., 2011; Browne and Sylla, 2012), of the influence of external forcing such as Sea Surface Temperature (SST, Paeth and A. Hense, 2004), dust (Konare et al., 2008; N'Datchoh et al., 2017) and land-use changes on the dynamic of the monsoon system (Abiodun et al., 2012; Zaroug et al., 2012).

RegCM versions (Giorgi et al., 2012; Pal et al., 2007) are the one of the most commonly used among the large range of RCMs to study the climate of West African and of many regions of the world. Compared with the previous version (RegCM3; Pal et al., 2007), the latest release

(RegCM4) has been improved with substantial development of the software code and of the physical representations (Giorgi et al., 2012) and with the introduction of CLM (version 3.5 and 4.5) as an option to describe land surface processes. Previously it was Biosphere-Atmosphere Transfer Scheme (BATS; Dickinson et al., 1993) only which was used as land surface model. Many studies have shown that the model performs well when using BATS over the West Africa (Sylla et al., 2009; Diallo et al., 2013) but CLM offers improvements in the land-atmosphere exchanges of moisture and energy and in the associated surface climate feedbacks (Steiner et al., 2009). Nonetheless it was shown over India that CLM use may lead to a weaker performance of RegCM than BATS (Halder and al. (2015. Thus, the performance of RegCM4 when using CLM (RegCM4-CLM4.5) needs to be assessed and sensitivities tests have to be conducted on physical processes parameterization to find the optimal configuration of the RCM for a given region and to give the relevant information to RCM users.

Among different physical processes in climate models, the convective parameterization is usually considered as the most important when simulating the monsoon rainfall (Im et al., 2008; Leung et al., 2004). Simulations of regional climate are very sensitive to physical parameterization schemes, particularly over the tropics where convection plays a major role in monsoon dynamics (Singh et al., 2011; Srinivas et al., 2013; Gao et al., 2016). One of the main sources of uncertainties in climate prediction is related to the representation of the clouds, which mainly influences the energy response of the models to a disturbance (Soden and Held, 2006; IPCC, 2007). Thus, implementing appropriate convective scheme in dynamic models is needed for realistic simulations.

Several sensitivity studies using previous version of RegCM have been conducted over Africa. Meinke et al. (2007) and Djiotang and Kamga (2010) showed that in West Africa, the monsoon precipitations are sensitive to the choice of cumulus parameterization and closure schemes. Brown and Sylla (2012) performed a sensitivity study of RegCM3 to the domain size over West Africa and showed that a large domain is required to capture variability of summer monsoon rainfall and circulation features. Recent study by Adeniyi (2014) using version 4 of RegCM indicated that all convective schemes give good spatial representation of rainfall with biases over West Africa. Komkoua and al. (2016) found that the last release of RegCM implementing Grell as convective scheme with Arakawa-Schubert closure assumption is more suitable to downscale the diurnal cycle of rainfall over Central Africa. However, none of these studies have attempted to investigate a sensitivity study of the Regional Climate Model (RegCM4) to the convective scheme over West Africa with CLM4.5 as the land surface model.

This study investigates the performance of RegCM4-CLM4.5 over West Africa using different convection schemes in the aim to identify the “best” configuration option for the region. It is worth noting that the few previous similar sensitivity studies conducted in the region was performed using BATS as land surface scheme and involved less convective schemes. The paper is structured as follows: the description of the model, data and numerical experiments used to investigate the RegCM4 performance are described in Section 2; Section 3 analyzes and discusses the model’s performance under different convection processes; and the main conclusions are summarized in Section 4.

2 Model description, observation datasets and numerical experiments

2.1 Model description and datasets.

The 4th generation of the ICTP RegCM (hereafter RegCM4) is used in this study. RegCM is a limited-area model using a terrain-following σ-pressure vertical coordinate system and an Arakawa B-grid finite differencing algorithm (Giorgi et al., 2012). The model’s dynamical component is derived from the hydrostatic version of the Pennsylvania State University Mesoscale Model version 5 (MM5; Grell et al., 1994) with improvements on the coupling with an advanced and complex land surface model (CLM3.5 and CLM4.5; Oleson et al., 2008 and 2013). In the version used here, the radiation scheme is derived from the NCAR global model CCM3 (Kiehl et al., 1996) and includes representation of aerosols following Solmon et al. (2006) and Zakey et al. (2006). Turbulent transports of momentum, water vapor and sensible heat in the planetary boundary layer over land and ocean are computed as Holtslag et al. (1990), which allows nonlocal transport in the convective boundary layer. The large-scale precipitation scheme of Pal et al. (2000) referred as SUBgrid EXplicit moisture scheme (SUBEX) includes the subgrid variability in clouds (Sundqvist and al., 1989) and the evaporation and accretion processes for stable precipitation. Ocean surfaces fluxes of momentum, heat and moisture are represented using the scheme of Zeng and al. (1998) with a drag coefficient-based bulk aerodynamic procedure and considering the influence of surface friction velocity on roughness length computed following Smith (1988) and Brutsaert (1982), respectively for momentum and heat (and also moisture).

The soil-vegetation-atmosphere interaction processes are parameterized using Community Land Model (CLM version 4.5; Oleson et al., 2013). CLM4.5 presents in each grid cell the possibility to have fifteen soil layers, up to five snow layers, five different land unit types and sixteen different plant functional types (Lawrence et al., 2011; Wang et al., 2016). RegCM4-CLM4.5 proposes five different convective schemes (Im et al., 2008; Giorgi et al., 2012): the modified-Kuo scheme (Anthes et al., 1987), the Tiedtke scheme (Tiedtke, 1989), the Emanuel scheme (Emanuel, 1991), the Grell scheme (Grell, 1993) and the Kain-Fritsch scheme (Kain-Fritsch, 1990; Kain, 2004) with the possibility to combine different schemes over ocean and land (called as 'mixed' convection).

2.2 Convective schemes

The convective precipitation parameterizations used in this study are Tiedke (1989), Emanuel (1991) and Grell (1993) schemes.

The Emanuel (1991) scheme assumes that the mixing in clouds is highly episodic and inhomogeneous (in contrary to a continuous entraining plume) and takes into account convective fluxes based on an idealized model of sub-cloud-scale updrafts and downdrafts. Convection is triggered when the level of neutral buoyancy is greater than the cloud base level. Between these two levels, air is lifted and a fraction of the condensed moisture forms precipitation while the remaining fraction forms the cloud. The cloud is supposed to mix with the air from the environment according to a uniform spectrum of mixtures that ascend or descend to their respective levels of neutral buoyancy. The mixing entrainment and detrainment rates depend on the vertical gradients of buoyancy in clouds. Emanuel scheme includes a formulation of the auto-conversion of cloud water into precipitation inside cumulus clouds.

In the Grell (1993) scheme, deep convective clouds are represented by an updraft and a downdraft that are undiluted and mix with environmental air only in cloud base and top. Heating and moistening profiles are derived from latent heat released or absorbed, linked with the updraft-downdraft fluxes and compensating motion (Martinez-Castro et al., 2006). Two types of Grell scheme convective closure assumption can be found in RegCM4. In the Arakawa–Schubert (1974) closure (AS), a quasi-equilibrium condition is assumed between the generation of instability by grid-scale processes and the dissipation of instability by sub-grid (convective) processes. In the Fritsch–Chappell (FC) closure (Fritsch and Chappell, 1980), the available buoyant energy is dissipated during a specified convective time period (between 30 min and 1 hour).

Similarly, the Tiedtke (1989) scheme is a mass flux convection scheme, albeit it considers a number of cloud types as well as cumulus downdrafts that can represent deep, mid-level and shallow convection (Singh et al., 2011; Bhatla et al., 2016). The closure assumptions for the deep and mid-level convection are maintained by large-scale moisture convergence, while the shallow convection is sustained by the supply of moisture derived from surface evaporation.

2.3 Numerical experiments and methodology

Five experiments using the convection schemes of (1) Emanuel over land and Grell over ocean (mix1), (2) Emanuel, (3) Grell, (4) Tiedtke and (5) Grell over land and Emanuel over ocean (mix2) are conducted using RegCM4-CLM4.5 with 18 sigma levels at 50 Km horizontal resolution for the period from November 2002 to September 2004. The two first months (i.e. November and December 2002) was considered as spin-up time and not included in the analysis. The years 2003 and 2004 has been selected in this study because they corresponded respectively to dry and wet year in this region. The analyses will focus on the rainy season from June to September (JJAS). As quantitative measurements of model skills, we consider mean bias (MB) which is the difference between the area-averaged value of the simulation and the observation, the spatial root mean square difference (RMSD) and the spatial correlation called Pattern Correlation Coefficient (PCC) and the distribution of Probability Density Function (PDF) of the temperature bias. The RMSD, PCC and the PDF provide information at the grid-point level while the MB does so at the regional level. A Taylor diagram (Taylor, 2001) is used to summarize assessments above and to show the deviation of different model configurations results from observations.

As assumed in Gao et al. (2016), the temperature bias in JJAS present a normal mode type of distribution. The PDF is expressed as:

$$\frac{1}{\sigma\sqrt{2\pi}} e \frac{(x-\mu)^2}{(2\sigma)^2} (1),$$

where μ is the mean and σ the standard deviation of temperature bias.

The PDF is characterized by its bell shaped curve, the temperature biases distribute symmetrically around the mean bias temperature value in decreasing numbers as one moves away from the mean. The empirical rule states that for a normal distribution, nearly all of the data will fall within three standard deviations of the mean. The empirical rule can be broken down into three parts:

- 68% of grid points fall within the first standard deviation from the mean.
- 95% of grid points fall within two standard deviations from the mean.
- 99.7% of grid points fall within three standard deviations from the mean.

The rule is also called the 68-95-99.7 Rule or the Three Sigma Rule. Thus, they constitute measurements of model performance and systematic model errors. These metrics are computed for each of the sub-regions indicated in Figure 1.

For this sensitivity study, the model was run at its standard configuration with 18 vertical sigma layers (model top at 50 hPa) and with initial and boundary conditions provided by the European

Centre for Medium Range Weather Forecasts reanalysis ERA-interim (Simmons et al., 2007; Uppala et al., 2008) at an horizontal resolution of 50 km and a temporal resolution of 6 hours (00:00, 06:00, 12:00 and 18:00 UTC). Sea-surface temperatures (SST) were from NOAA optimal interpolation weekly SST data (Reynolds et al., 2007). The terrain characteristics (topography and land use data) were derived from United States Geological Survey (USGS) and Global Land Cover Characterization (GLCC; Loveland et al., 2000) respectively at 10 min horizontal resolution.

We focus our analysis on the precipitation and on the air temperature at 2m in the summer of June-July-August-September (JJAS) over mainland West Africa. To reduce uncertainty due to lack of surface climate observations over the region (Nikulin et al., 2012; Sylla et al., 2013a), the simulated precipitation is validated using two observational datasets : the GPCP product (1°×1° resolution) is a satellite-derived dataset developed under the Global Precipitation Climatology Project and made available from late 1996 to present and the 0.25° high resolution dataset of Tropical Rainfall Measuring Mission 3B43V7 (TRMM) available from 1998 to 2013 (Huffman et al.2007). The simulated 2m temperature is validated using also two observational datasets including the Climate Research Unit (CRU) time series version 3.20 gridded at 0.5° horizontal resolution from the University of East Anglia and available respectively from 1901 to 2011 (Harris et al., 2013), and the University of Delaware version 3.01 (UDEL) gridded dataset at 0.5° horizontal resolution available from 1900 to 2010 (Legates and Willmott, 1990). The simulated atmospheric fields are compared with ERA-Interim reanalysis available from 1979 to present at 1.5° horizontal resolution (Dee et al., 2011). All products have been regridded to 0.44°×0.44° using a bilinear interpolation method to facilitate the comparison with RegCM4 simulations (Nikulin et al., 2012). The model's performance is further examined in four sub-regions (Fig. 1), each with different characteristics of the annual cycle of rainfall: Central Sahel (10°W–10°E; 10°N–16°N), West Sahel (18°W–10°W; 10°N–16°N), Guinea Coast (15°W–10°E; 3°N–10°N) and West Africa (20°W–20°E; 5°S–21°N).

3 Results and discussion

3.1 Temperature

The spatial distribution of averaged temperature during JJAS over 2003-2004 from CRU and UDEL observations (resp. Fig. 2a, b) is compared to the temperature simulated by RegCM4 using the convection schemes: Mix1, Emanuel, Grell, Tiedtke and Mix2 (resp. Fig. 2c-g). Figure 3 shows the associated mean model biases with areas statically significant at 95% of confidence level (The dotted area denotes differences which are statistically significant at a significance level of 0.05) relatively to CRU for observation (UDEL; Fig.3a) and the model simulations (Fig. 3b-f). Table 1 reports the PCC and the RMSD between the simulated and observed temperature calculated for Guinea Coast, Central Sahel, West Sahel and the entire West Africa domain.

The CRU temperatures presents a zonal distribution in West Africa with maximum (>34°C) in the Sahara and lowest temperatures (< 22°C) over the Guinea Coast and over complex terrains such as the Jos plateau, Cameroon mountains and Guinean highlands. The Figure 3 show that the spatial distribution of the temperature biases is statically significance at 0.05 levels over most of the domain study. Except over the Guinea coast region and Cameron Mountains. The UDEL observation (Fig. 2b) shows similarity with CRU in terms of spatial distribution with PCC larger than 0.98 over the entire West African domain (see Table 1). However, UDEL depicts a sparse distribution with a mixture of warm and cold bias over the Sahara and along of Nigeria/Cameroon border around ±2°C (see Fig. 3a). There is also a good agreement between model simulated temperatures and CRU observation with the PCCs more than 0.93 (Table 1) over West Africa. All model configurations well reproduce the general features of the observed pattern including the meridional surface temperature gradient zone between Guinea Coast and the Saharan desert. This temperature gradient is important for the evolution of the African Easterly Jet (AEJ) (Cook 1999; Thorncroft and Blackburn, 1999). All model configurations (Fig. 3b-d, f) exhibit a similar dominant cold biases except the Tiedtke configuration (Fig. 3e) in the Sahara desert at the central part of Mauritania and Niger, and along the Guinea Coast region. The greater cold bias with value up to -5°C occurs when using Grell configuration while, simulation using Tiedtke configuration depicts a dominant warm bias up to 4°C mainly located in Central Sahel around 12°N (Fig. 3e). One effect of the warm bias shown in Tiedtke simulation is to shift the zone of meridional temperature gradient southward relative to its observed position (Fig. 2f). However, it is difficult to determine the origin of RCM temperature biases as they involve changes in surface-atmosphere interactions and as they are function of many factors such as surface albedo, cloudiness, temperature advection and surface water and energy fluxes (Tadross et al., 2006; Sylla et al., 2012).

For a quantitative evaluation of the performance of these sensitivity tests, the PDF statistical tool was used. The PDF distributions of the temperature bias in JJAS is shown in Figure 4 for Guinea Coast, Central Sahel, West Sahel and the entire West Africa domain. The PDF distribution shows a general dominant cold bias (see Fig. 4a-d) in model simulations over most of study domain, except with Tiedtke configuration in the Central Sahel region.

Over Guinea Coast region, Grell configuration presents a colder bias with the maximum of temperature bias distribution centered around -2°C (see Fig. 4a) compared to the other configurations. However, Emanuel simulation shows the lower RMSD about 1.29°C with a PCC larger than 0.77 (see Table 1). For Central Sahel region (Fig. 4b) a warmer bias is found in Tiedtke simulation, while a colder bias is found in Grell and Mix2 configurations (see Fig. 4b). Emanuel configuration shows a lower value of RMSD about 0.67°C and a higher PCC larger than 0.95 compared to the other model simulated temperatures (see table 1). In West Sahel a colder bias is found with Grell scheme (see Fig. 4c) while Emanuel and Tiedtke simulations show a mixture of cold and warm bias. Configuration of RegCM with Emanuel presents a better performance with a lower RMSD and higher PCC values compared to the other simulations in West Sahel. Over the entire West Africa domain (see Fig.4d), Grell and Tiedtke present respectively a colder and warmer bias. Generally, with respect to temperature simulations, a better performance of RegCM4 is obtained when using Emanuel scheme.

3.2 Precipitation

The spatial distribution of mean JJAS precipitation (2003–2004) over West Africa is shown in Figure 5 for observations GPCP and TRMM (resp. Fig. 5 a-b) and for RegCM4 simulations with the following convective schemes Mix1, Emanuel, Grell, Tiedtke and Mix2 (resp. Fig.5 c-g). Sylla et al. (2013a) argued that over Africa, GPCP is more consistent with gauge based observations, whilst Nikulin et al. (2012) found a significant dry bias over tropical Africa in TRMM compared to GPCP. We therefore select, for precipitation, GPCP as our main observational reference in this paper. Figure 6 shows the corresponding precipitation mean biases with statically significant at 95% of confidence level (The dotted area denotes differences which are statistically significant at a significance level of 0.05) relatively to GPCP for TRMM (Fig 6a) and for the different simulations configurations (Mix1, Emanuel, Grell, Tiedtke and Mix2; Fig 6b-f respectively). GPCP depicts a zonal band of rainfall decreasing from North to South (see Fig. 5a). Precipitation maxima are found in orographic regions of Guinea highlands, Jos Plateau, and Cameroon Mountains. The Figure 6 show that the spatial distribution of the precipitation biases is statically significance at 0.05 levels over almost the domain study. Differences between TRMM and GPCP observation products (Table 2) can reach up to -5.26% at sub-regional levels, while over the entire West Africa it does not exceed 0.82%. Although both observation products exhibit some differences (Fig.6a), their patterns show a good agreement, with PCCs more than 0.96 over the entire West Africa domain (Table 2). TRMM underestimates the rainfall intensity over Guinea Coast and Central Sahel regions (respectively no more than -0.86% and -5.12%) and overestimates the rainfall intensity over West Sahel and the entire West Africa domain reaching respectively 3.48% and 0.83%. The spatial distribution of rainfall is well reproduced by all model configurations with PCCs values within the range 0.61 and 0.89 over the entire West African domain. The dominant feature in these simulations is the dry bias over West Africa domain (Fig. 6b-f), which is more pronounced in the Tiedtke configuration (see Table 2). The warmer bias over Central Sahel in Tiedtke configuration (Fig.3e) is consistent with the drier bias found in the same region (see Table 2 and Fig.6e), as less rainfall would induce less evaporative cooling (decrease of latent heat flux) and therefore less favorable conditions for cloud cover (Feddema et al. 2005). The decrease of the cloud cover will lead to an increase of incident radiation inducing an increase of sensible heat flux and warmer surface temperatures. Moreover, a drier bias may be associated with a heating induced by the adiabatic subsidence to compensate effect of the increase of the surface albedo (Charney 1975). However, the Table 2 reveals that Mix1 and Emanuel show a better performance with a lower mean biases and greater PCC compared to the other model simulations over the entire West African domain and its sub-regions.

In order to understand the origins of the model rainfall biases, we analyzed the JJAS midlevel (850–300 hPa) vertically integrated water vapor mixing ratio and the 650 hPa low-level wind (African Easterly jet, AEJ) over West Africa averaged over the 2003–2004 period (Fig. 7). The AEJ is the most prominent feature affecting the West African Monsoon through its role in organizing convection and precipitation over the region (Cook, 1999; Diedhiou et al., 1999; Mohr and Thorncroft, 2006; Sylla et al., 2011). Areas with larger water vapor mixing ratio corresponds to the areas of maximum precipitation in observations (see Fig. 5a-b). Around 9°N the weaker easterly wind (AEJ) contributes to enhance the moisture convergence which results in an increase of water vapor and precipitation (see Fig. 5a-b). All model configurations show some quantitative differences compared to ERA-Interim in both the wind flux and the water vapor mixing ratio.

The underestimation of vertically integrated water vapor mixing ratio is larger in Grell and Mix2 simulations (Fig. 7 c, e) over the Guinea Coast and Atlantic Ocean compared to those of Mix1, Emanuel and Tiedtke (Fig. 7 a, b, e). Mix1 and Emanuel configurations reproduce better the spatial extent of the moisture convergence than the other model configurations (Fig.7b, c). All model configurations simulate a stronger easterly wind flux (AEJ) than observed in particular over the Guinea Coast and Atlantic Ocean inducing a negative impact on simulated precipitations in the sub-regions (see Fig. 5c–g). Another possible explanation of model rainfall biases is further discussed in Brown and Sylla (2011) whereby a sensitivity study on the domain size with RegCM3 over West Africa showed that RegCM3 simulates drier conditions over a default domain (RegCM-D1) quite similar to our domain size used in this study.

A Taylor diagram is used to give a combined synthetized view of the pattern correlation coefficient and the JJAS standard deviation of precipitation from the different sensitivity studies with respect to GPCP over Guinea Coast, Central Sahel, West Sahel and West Africa. Model standard deviations are normalized by the observed value from GPCP (indicated by REF, see Fig.8). For the entire West Africa domain, the diagram shows Tiedtke and Emanuel outperform the other configurations with values of standard deviation normalized much closer to 1. However Emanuel configuration present a better spatial correlation reaching 0.8 as compared to Tiedke configuration. Over Guinea Coast sub-region Grell and Emanuel present better values of standard deviation normalized. However, in regarding the spatial correlation value about 0.7 Emanuel configuration is the best. For West and Central Sahel, Mix1 and Emanuel are closer to observation. However, Emanuel outperforms Mix1 configuration with a good spatial correlations scores between 0.7 and 0.8 respectively over Central and West Sahel sub-regions. From the Taylor diagram, it can be inferred that Emanuel performs better regarding the standard deviation normalized and the pattern correlation over the entire West African domain and its sub-regions.

Based on previous experience and studies, Gao and al. (2016) noted that use of the Emanuel convection scheme in RegCM3 and RegCM4 over China tends to simulate too much precipitation when using BATS as the land surface scheme. They explained that it is mainly due to the fact that the Emanuel scheme responds quite strongly to heating from the surface land as compared to Grell and Tiedtke convection schemes, once convection is triggered. BATS with only two soils levels depth maximizes this response; this is why Emanuel is too wet when using BATS as compared to Grell and Tiedtke. By contrast, CLM uses several soil layers down to a depth of several meters; therefore, the upper soil temperatures respond less strongly to the solar heating. Precipitation amount is much reduced when using CLM, which is good for Emanuel but not good for Grell and Tiedtke (Gao and al., 2016) while the combination of BATS with Grell and Tiedtke shows good performance (Gao et al., 2012; Ali et al., 2015).

In conclusion, although RegCM4-CLM4.5 shows some weaknesses, such as a dry bias over most of Central Sahel and Guinea Coast region, its performance in replicating the spatial distribution of rainfall appears in line with that documented in previous studies using the previous version RegCM3 (Sylla et al., 2009; Abiodun et al., 2012).

3.3 Mean annual cycle

In this section, we examine the effect of the convection scheme in the characterization of the three distinct phases of the West African Monsoon: the onset, the high rain period and the southward retreat of the monsoon rain band (Sultan et al., 2003). Such behavior is best represented by a meridional cross-section (time-latitude Hovmoller diagram). This diagram provides a robust framework to assess RCM's skills in simulating seasonal and intraseasonal variations of the WAM, and thus the mechanisms of the region's rainfall (Hourdin et al., 2010). Figure 9 shows the time-latitude diagrams of rainfall averaged over the region between 10°E and 10°W for observations GPCP and TRMM (resp. Fig 9a-b) and for model simulations using Mix1, Emanuel, Grell, Tiedtke and Mix2 convection schemes (resp. Fig 9c-g). The averages are taken for the period 2003–2004 and displayed throughout the year. This figure shows that the cores of the different phases are well marked in TRMM than in GPCP (resp. Fig.9a, b). TRMM observation shows a first rainy season from mid-March up to mid-June over the Gulf of Guinea and Guinea Coast with a northward extension of the rain belt up to about 5°N (Fig.9b). The monsoon jump is characterized by a sudden cessation of precipitation intensities (Sultan and Janicot, 2000, 2003) and occurs from mid-June to early July, when the rain band core moves suddenly northward to about 10°N (Fig.9b). This indicates the beginning of the rainy season over the Sahel with a peak reached in August between 9° and 12°N over Central Sahel. A gradual retreat of the monsoon starts in end of August and it is well shown by GPCP (Fig.9a), with a decrease in intensity and a southward migration of the rain band. There are both similarities and differences across the two observation datasets TRMM and GPCP. Both datasets agree in area of rainfall maximum intensity around 4°N despite a more intense peak of rainfall for TRMM compare to GPCP (resp. Fig.9a, b). The monsoon jump characterized by a discontinuity sharp is not well defined in GPCP compared to TRMM. In addition, GPCP shows wet conditions during the retreat phase in July to September compared to TRMM (Fig.9a, b).

Mix1, Emanuel, and Grell model configurations (resp. Fig.9c-e) capture the three phases of the seasonal evolution of the WAM, while Tiedke and Mix2 simulations fail to reproduce them in particular the rainy season over Central Sahel. However Emanuel and Mix model configurations (resp. Fig. 6c, d) overestimate rainfall amounts during the two rainy seasons over Guinea Coast, mostly as a result of an overestimate of the precipitation over the orographic regions of Guinea highlands, Jos Plateau, and Cameroon Mountains. Mix1 and Mix2 configurations are respectively wetter and drier compared to the other model configurations (resp. Fig. 9c, g). Generally, the three monsoon phases are well shown by Grell simulation, albeit it is drier compared to the other model simulations.

Another analysis of the annual cycle consists of considering the area-averaged (land-only grid points) value of monthly rainfall and temperature over the Gulf of Guinea, the Central Sahel and the entire West African domain (Figures 10 and 11). This allows better identification of rainfall and temperature minima and peaks. Figure 10a-d shows respectively the annual cycle of precipitation averaged over Guinea Coast, Central Sahel, West Sahel and the entire West African domain. Over the Guinea Coast (Fig 10a), both GPCP and TRMM observations show a primary maximum in June and a secondary one in September. The Mix1 and Tiedtke model configurations simulate an early first peak in May while Emanuel, Grell and Mix2 configurations well capture the observed peak in June. We note that all model configurations well reproduce the timing of the mid-summer break and second rainfall peak in September but they underestimate its magnitude, although Mix1 simulation result is higher and much closer to observations compared to the other model simulations.

In both Central Sahel and West Sahel, observations (GPCP and TRMM) display a dry spring (from January to March) and winter (from October to December) and a wet summer (from June to September) with a well-defined peak occurring in August. Model configurations reproduce both phase of the annual cycle and the observed rainfall peak in August except Emanuel configuration which shifts it in September over West Sahel region. Model simulations underestimate the peak intensity compare to observations. However Mix1 configuration rainfall peak is much closer to observation for both Central Sahel and West Sahel regions (resp. Fig 10b, d) compared to the other model simulations. Over the entire West African domain, the annual cycle (Fig 10c) is smoother with a notable shift of the peak in September in the different model configurations. All the model configurations underestimate the rainfall peak and shift it in October. However, Mix1 and Emanuel model simulations are much closer to observed annual cycle of precipitation compared to the others. In resume Mix1 simulation compared to the others better reproduces the observed annual cycle of precipitation over the sub-regions and the entire West African domain.

The annual cycles of temperature for Central Sahel, West Sahel and the entire West African domain of Mix1, Emanuel, Grell, Tiedtke and Mix2 convection schemes are shown in Figure 11b-d. The observations (CRU and UDEL) indicate a cooler winter from December to February and warmer pre and post-monsoon periods with relative minima occurring during August. While over Guinea Coast, both winter and post monsoon are cooler and only the pre monsoon phase is warmer (Fig. 11a). Models configurations present similar seasonal variation of the mean monthly temperature at 2 m compared to observations, but do exhibit some differences.

Over Guinea Coast model simulations underestimate the magnitude of the temperature compared to observations. However, Tiedtke configuration is higher and much closer to observations compared to the other model simulations throughout the year (Fig.11a). Over Central Sahel region, Grell and Tiedtke capture well the seasonal variation from November to June in particular the first peak in August compared to the other models simulations. During the summer (JJAS) Emanuel and Mix1 quite well reproduce the observed precipitation annual cycle (Fig.11b). Therefore, model simulations underestimate the seasonal variation of temperature over the entire West African domain. Although Tiedtke simulation overestimates the mid-summer break period, it is much closer to observed annual cycle of temperature throughout the year compared to the other model simulations. Over the West Sahel, model simulations quite well reproduce the annual cycle of temperature except Grell and Mix2 configurations in particular during the summer (JJAS). In summary Tiedtke simulation better reproduces the observed annual cycle of temperature throughout the year over the sub-regions and the entire West African domain compared to the other model configurations.

The divergences in the RCMs annual cycles arise mostly from their different abilities to simulate the main features responsible of triggering and maintaining the WAM precipitation (Gbobaniyi E. et al., 2013). Among them, we have the monsoon flow, the African Easterly Jet (AEJ), the Tropical Easterly Jet (TEJ) and the Africa Easterly Waves (AEWs) (Diedhiou et al., 1999; Sylla et al., 2013b). .

3.4 Wind profile

The atmospheric circulations and their interactions with ITCZ play an important role in the WAM system (Nicholson, 2013). Thus, this section aims to analyze the impact of the choice of convection scheme in the simulations of zonal winds features, including the near-surface westerly component (the West African Monsoon, WAM), the African Easterly Jet (AEJ) and the Tropical Easterly Jet (TEJ) in the mid and upper troposphere respectively. Figure 12 depicts the vertical cross section of the JJAS mean of the zonal wind averaged between 10°W and 10°E for ERA-Interim (Fig.12a) and model configurations in Mix1, Emanuel, Grell, Tiedtke and Mix2 convection schemes (resp. Fig.12 b-f). The reanalyse ERA-Interim (Fig. 12a) displays the monsoon flow winds below 800 hPa at 2-18°N with two cores merged over both Guinea Coast (centered at 6°N) and Central Sahel (centered at 15°N) sub-regions, the AEJ in the mid-levels centered at 12°N and the TEJ in the upper tropospheric levels at 200 hPa centered at 5°N (Fig12 a). All model configurations well reproduce the zonal wind features despite some biases.

Model simulations Mix1, Emanuel, Grell and Tiedtke present a strong core of monsoon flow compared to Era-Interim (reaching 6m/s). The stronger and weaker monsoon flows are found with Mix1 and Mix2 configurations respectively compared to the other configurations. However, model simulations well reproduce the limit of the surface westerly flow compared to its position. Of particular interest is the core of the AEJ in the mid-tropospheric levels, which is greatly weakened with Mx1 and Emanuel. While AEJ magnitude core is well defined in Grell and Mix2 simulations at 12°N, but its spatial extent is somewhat reduced. This location of the AEJ in Grell and Mix2 simulation is consistent with the location of the region of zonal temperature gradient (see resp. Fig. 3e, g), as the AEJ is associated with the surface temperature gradient (Cook, 1999; Thorncroft and Blackburn, 1999). While Tiedtke simulation shifts the location of AEJ core at 8°N in agreement with the warm bias shown in Tiedtke configuration (see Fig.4e). The TEJ at 200 hPa and 5°N is very similar in model simulations compared to the ERA-Interim reanalysis. However, the core of the jet is weaker in Tiedtke configuration compared to the other model simulations. An overall, Grell configuration outperforms simulations of the main features of the zonal wind compared to the other model simulations.

4 Summary and conclusion

The latest released RegCM4 have been performed over West Africa for two years (2002-2003) to assess its performance using five convective parameterizations: (a) the Emanuel scheme, (b) Emanuel over land and Grell over Ocean (Mix1), (c) the Grell scheme, (d) the Tiedke scheme and (e) Grell over land and Emanuel over Ocean scheme (Mix2). The sensitivity of the model to different convection schemes were validated using observations. The main findings and conclusions can be summarized as follows:

(1) Compared with the previous version of RegCM, RegCM4-CLM also shows a general cold bias over West Africa. However in Central Sahel region, Tiedtke simulation presents a warm bias. This warms bias tends to displace the meridional temperature gradient southward relative to its observed position. An overall, with respect to temperature, better performance are obtained when using Emanuel scheme.

(2) With respect to the precipitation, the dominant feature in model simulations is a dry bias which is more pronounced when using Tiedtke convection scheme. Considering the good performance over the entire West Africa domain and its sub-regions in the temperature and precipitation simulations, we suggest Emanuel convection scheme when using RegCM4-CLM4.5 over West Africa.

(3) Simulations when using Mix1 and Emanuel schemes well reproduce the spatial extent of moisture convergence of the ERA-Interim reanalyses compared to the other convection schemes. However, in the mid-levels of the atmosphere, model simulations show an easterly wind flux (AEJ) stronger than observed in particular over the Guinea Coast and Ocean Atlantic below the latitude 4°N, creating an increased subsidence and has a negative effect on simulated precipitations there. This is a possible explanation of a dry bias over West Africa domain. However, the vertical features of the zonal wind, including the near-surface westerly component, the AEJ and the TEJ in the mid and upper troposphere are better simulated when using Grell convection scheme compared to the other model simulations

(4) The time evolution of simulation when using Grell convection scheme rainfall matches well with the observed evolution, including the timing of the discontinuous northward jump of the main rainfall band in late June, albeit it is drier compared to Mix1 and Emanuel convection scheme.

(5) Over Central Sahel and West Sahel, the mean annual cycle of precipitation and temperature, with the single peaked rainy season is especially well captured in terms of timing despite the fact that all model simulations underestimated the magnitude. However, simulations using Mix1 reproduce better the annual cycle of precipitation compared to the other schemes.

(6) Over Guinea Coast, Mix1 and Tiedtke model simulations failed to reproduce the double peaks rainy seasons, while Emanuel, Grell and Mix2 simulations well reproduce them but underestimate their amplitude. The bimodal nature of rainfall associated with the Guinea sub-region is not so well defined when averaging rainfall over the entire West African domain. This emphasizes the importance of separating regions into homogeneous precipitation sub-regions for evaluation analyses.

(7) The mean annual cycle of temperature is well reproduce in simulation when using Tiedtke convection scheme throughout the year over the sub-regions and the entire West Africa domain compared to the other model simulations.

As more advanced package compared to the previously version of RegCM with BATS, CLM4.5 can be considered as the primary land surface processes option in RegCM4. Therein, the use of Emanuel scheme is recommended over the West African region. We plan to use this configuration in long-term multi-decadal simulations to further evaluate the model capability in reproducing the mean climatology. To bring up this study more complete, we will study the sensitivity of temperature and precipitation extremes simulated by RegCM4-CLM4.5 to different convective schemes.

Acknowledgements

This work is dedicated to the memory of Prof Abdourahamane Konaré with whom we started this assessment. The authors thank the Institute of Research for Development (IRD, France) and Institute of Geosciences for Environment (IGE, University Grenoble Alpes) for providing the facility (the Regional Climate Modelling Platform) to perform these simulations and the IT support funded by IRD/PRPT contract at the University Felix Houphouet Boigny (Abidjan, Côte d'Ivoire). The authors are grateful to all students, technicians, engineers and researchers involved at ICTP (Abdus Salam International Centre of Theoretical Physics; Trieste, Italy) on the development and the improvement of the regional climate model RegCM. The research leading to this publication is co-funded by the NERC/DFID "Future Climate for Africa" programme under the AMMA-2050 project, grant number NE/M019969/1 and by IRD (Institut de Recherche pour le Développement; France) grant number UMR IGE Imputation 252RA5".

References

Abiodun BJ, Adeyewa ZD, Oguntunde PG, Salami AT, Ajayi VO. 2012. Modeling the impacts of reforestation on future climate in
West Africa. Theor. Appl. Climatol. 110(1–2): 77–96.

Adeniyi MO. 2014. Sensitivity of different convective schemes in RegCM4.0 for simulation of precipitation during the Septembers of 1989 to 1998 over West Africa. Theor. Appl. Climatol. 115(1–2): 305–322, doi: 10.1007/s00704-013-0881-5.

Adler RF et al (2003). The version-2 Global Precipitation Climatology Project (GPCP) monthly precipitation analysis (1979–present). J Hydrometeorol 4(6):1147–1167

Ali S., L. Dan, C. B. Fu, and Y. Yang, 2015: Performance of convective parameterization schemes in Asia using RegCM: Simulations in three typical regions for the period 1998–2002. Adv. Atmos. Sci., 32(5), 715–730, doi:10.1007/s00376-014-4158-4.h

Arakawa A, Schubert WH (1974) Interaction of a cumulus cloud ensemble with the large scale environment. Part I. J Atmos Sci 31: 674–701

Bhatla R., S. Ghosh, B. Mandal, R.K. Mall, Kuldeep Sharma. "Simulation of Indian summer monsoon onset with different parameterization convection schemes of RegCM-4.3", Atmospheric Research, 2016. DOI : 10.1016/j.atmosres.2016.02.010

Browne N.A.K., Sylla MB. 2012. Regional climate model sensitivity to domain size for the simulation of the West African monsoon rainfall. Int. J. Geophys. Article ID 625831, DOI: 10.1155/2012/625831.

Brutsaert W (1982) Evaporation into the atmosphere: theory, history and applications. USA: Reidel Himgham Mass, 299 pp

Charney, J. G. (1975). Dynamics of deserts and drought in the Sahel. Quarterly Journal of the Royal Meteorological Society, 101(428), 193-202.

Cook, K. H., 1999: Generation of the African easterly jet and its role in determining West African precipitation. J. Climate, 12, 1165–1184, doi:10.1175/1520-0442(1999)012,1165:GOTAEJ.2.0.CO;2.

Dee et al (2011) The ERA-Interim reanalysis: configuration and performance of the data assimilation system. Quat J R Meteorol Soc 137:553–597. doi:10.1002/qj.828

Diallo I, Sylla MB, Camara M, Gaye AT. 2012. Interannual variability of rainfall and circulation features over the Sahel based on multiple regional climate models simulations. Theor. Appl. Climatol. DOI:10.1007/s00704-012-0791-y.

Diallo I, Sylla MB, Camara M, Gaye AT (2013) Interannual variability of rainfall over the Sahel based on multiple regional climate models simulations. Theor Appl Climatol. doi:10.1007/s00704-012-0791-y

Dickinson, R., A. Henderson-Sellers, and P. Kennedy. 1993. “Biosphere-Atmosphere Transfer Scheme (BATS) Version 1eas Coupled to the NCAR Community Climate Model.” NCAR Technical Note, NCAR/TN-387+ STR, 72 pp.

Diedhiou, A., Janicot, S., Viltard, A., De Felice, P., & Laurent, H. (1999). Easterly wave regimes and associated convection over West Africa and tropical Atlantic: Results from the NCEP/NCAR and ECMWF reanalyses. Climate Dynamics, 15(11), 795-822.

Djiotang Tchotchou LA, Mkankam Kamga F. 2010. Sensitivity of the simulated African monsoon of summers 1993 and 1999 to convective parameterization schemes in RegCM3. Theor. Appl. Climatol. 100: 207–220.

Emanuel, K. 1991. “A Scheme for Representing Cumulus Convection in Large-Scale Models.” Journal of the Atmospheric Sciences 48: 2313-2329.

Emanuel KA, Zivkovic-Rothman M (1999) Development and evaluation of a convection scheme for use in climate models. J Atmos Sci 56:1766–1782

Feddema, J. J., Oleson, K. W., Bonan, G. B., Mearns, L. O., Buja, L. E., Meehl, G. A., & Washington, W. M. (2005). The importance of land-cover change in simulating future climates. Science, 310(5754), 1674-1678.

Fritsch JM, Chappell CF (1980) Numerical prediction of convectively driven mesoscale pressure systems. Part I: Convective parameterization. J Atmos Sci 37: 722–1733

Gao, X., Y. Shi, D. Zhang, J. Wu, F. Giorgi, Z. Ji, and Y. Wang. 2012. "Uncertainties in Monsoon Precipitation Projections over China: Results from Two High-Resolution RCM Simulations." Climate Research 52: 213–226.

Gao Xue-Jie, Ying SHI, Filippo GIORGI, (2016). Comparison of convective parameterizations in RegCM4 experiments over China with CLM as the land surface model. Atmospheric and Oceanic Science Letters, 9:4, 246-254, DOI: 10.1080/16742834.2016.1172938

Gbobaniyi E, Sarr A, Sylla MB, Diallo I, Lennard C, Diedhiou A et al (2013) Climatology, annual cycle and interannual variability of precipitation and temperature in CORDEX regional climate models simulation overWest Africa. Inter J Climatol. doi:10.1002/joc.3834

Giorgi F, Coppola E, Solmon F, Mariotti L, Sylla MB, Bi X, Elguindi N, Diro GT, Nair V, Giuliani G, Cozzini S, Guettler I, O'Brien T, Tawfik A, Shalaby A, Zakey AS, Steiner A, Stordal F, Sloan L, Brankovic C. 2012. RegCM4: model description and preliminary tests over multiple CORDEX domains. Climate Res. 52: 7–29, DOI:v10.3354/cr01018.

Grell G, Dudhia J, Stauffer DR (1994) A description of the fifth generation Penn State/NCAR Mesoscale Model (MM5). National Center for Atmospheric Research Tech Note NCAR/TN-398+STR, NCAR, Boulder, CO

Grell, G. 1993. "Prognostic Evaluation of Assumptions Used by Cumulus Parameterizations." Monthly Weather Review 121: 764-787.

Halder S., Dirmeyer P. and K. Saha, 2015. "Sensitivity of the Mean and Variability of Indian Summer Monsoon to Land Surface Schemes in RegCM4: Understanding Coupled Land-Atmosphere Feedbacks." Journal of Geophysical Research 120:9437–9458

Harris I, Jones PD, Osborn TJ, Lister DH (2013) Updated high-resolution grids of monthly climatic observations. Int J Climatol. doi:10.1002/joc.3711

Holtslag A, De Bruijn E, Pan H-L (1990) A high resolution air mass transformation model for short-range weather forecasting. Mon Wea Rev 118: 1561–1575

Huffman GJ, Adler RF, Bolvin DT, Gu G, Nelkin EJ, Bowman KP, Hong Y, Stocker EF, Wolff DB (2007) The TRMM multisatellite precipitation analysis: quasi-global, multi-year, combined-sensor precipitation estimates at fine scale. J Hydrometeorol 8:38–55

Hourdin F, Musat I, Guichard F, Ruti PM, Favot F, Filiberti MA, Pham M, Grandpeix JY, Polcher J, Marquet P, Boone A, Lafore JP, Redelsperger JL, Dell'aquila A, Doval TL, Traore AK, Gall´ee H. 2010. AMMA-model intercomparison project. Bull. Am. Meteorol.Soc. 91(1): 95–104.

Im, E., J. Ahn, A. Remedio, and W.-T. Kwon. 2008. "Sensitivity of the Regional Climate of East/Southeast Asia to Convective Parameterizations in the RegCM3 Modelling System. Part 1: Focus on the Korean Peninsula." International Journal of Climatology 28: 1861–1877.

IPCC. 2007. Climate Change 2007: The Physical Science Basis. Contribution of Working group I to the Fouth Assessment Report of the Intergovernmental Panel on Climate Change, Solomon S, Qin D,Manning M, Chen Z, Marquis M, Averyth KB, Tignor M, Miller HL (eds). Cambridge University Press: Cambridge, UK, 996 pp.

Janicot S, Caniaux G, Chauvin F, de Coetlogon G, Fontaine B, Hall N, Killadis G, Lafore J-P, Lavaysse C, Lavender SL, Leroux S, Marteau R, Mounier F, Philippon N, Roehrrig R, Sultan B, Taylor CM (2011) Intraseasonal variability of the West African monsoon. Atmos Sci Lett 12:58–66. doi:10.1002/asl.280

Kain, J. S., and J. M. Fritsch, 1990: A one-dimensional entraining/detraining plume model and its application in convective parameterization. J. Atmos. Sci., 47, 2784–2802.

Kain J. S, 2004. The Kain–Fritsch Convective Parameterization: An Update. Journal of Applied Meteorology. Vol. 43, Issue 1, pp.170-181.

Kamga Foamouhoue A, Buscarlet ´ E. 2006. Simulation du climat de l'Afrique de l'Ouest à l'aide d'un modèle climatique régional: validation sur la période 1961–1990.

Komkoua Mbienda A. J., Tchawoua C., Vondou D. A., Choumbou P., Kenfack Sadem C., and Dey S, 2016. Sensitivity experiments of RegCM4 simulations to different convective schemes over Central Africa. Int. J. Climatol. DOI: 10.1002/joc.4707

Kiehl JT Hack JJ, Bonan GB, Boville BA, Briegleb BP, Williamson DL, Rasch PJ (1996) Description of the NCAR Community Climate Model (CCM3). Technical Note NCAR/TN—420+STR, p 152

Konare A, Zakey AS, Solmon F, Giorgi F, Rauscher S, Ibrah S, Bi X. 2008. A regional climate modeling study of the effect of desert dust on the West African monsoon. J. Geophys. Res. 113(D12): D12206.

Meinke I, Roads J, Kanamitsu M. 2007. Evaluation of RSM-simulated precipitation during CEOP. J. Meteorol. Soc. Jpn. 85A: 145–166.

Mohr, K. I., and C. D. Thorncroft, 2006: Intense convective systems in West Africa and their relationship to the African easterly jet. Quart. J. Roy. Meteor. Soc., 132, 163–176, doi:10.1256/qj.05.55.

N'Datchoh E. T. , Diallo I., Konaré A., Silué S., Ogunjobi K.O., Diedhiou A., Doumbia M. (2017) Dust induced changes on theWest African summer monsoon features. Int J Climatol, DOI: 10.1002/joc.5187.

Nicholson SE (2013) The West African Sahel: a review of recent studies on the rainfall regime and its interannual variability. Meteorology. Volume 2013, Article ID 453521, 32 pages. doi:10.1155/2013/453521

Nikulin G, Jones C, Samuelsson P, Giorgi F, Asrar G, Bu¨chner M, Cerezo-Mota R, Christensen OB, De´que´ M, Fernandez J, Hansler A, van Meijgaard E, Sylla MB, Sushama L (2012) Precipitation climatology in an ensemble of CORDEX-Africa regional climate simulations. J Clim 6057–6078. doi:10.1175/JCLI-D-11-00375.1

Lawrence, D. M., et al. (2011), Parameterization improvements and functional and structural advances in version 4 of the Community Land Model, J. Adv. Model. Earth Syst., 3, M03001, doi:10.1029/2011MS000045.

Legates DR, Willmott CJ (1990) Mean seasonal and spatial variability in gauge-corrected, global precipitation. Int J Climatol., 10:111–127

Leung, L., S. Zhong, Y. Qian, and Y. Liu. 2004. "Evaluation of Regional Climate Simulations of the 1998 and 1999 East Asian Summer Monsoon Using the GAME/HUBEX Observational

Loveland TR, Reed BC, Brown JF, Ohlen DO, Zhu J, Yang L, Merchant JW (2000) Development of a global land cover characteristics database and IGBP DISCover from 1-km AVHRR Data. Int J Remote Sensing 21: 1303–1330

Martinez-Castro, D., da Rocha, R. P., Bezanilla-Morlot, A., Alvarez-Escudero, L., Reyes-Fernández, J. P., Silva-Vidal, Y., & Arritt, R. W. (2006). Sensitivity studies of the RegCM3 simulation of summer precipitation, temperature and local wind field in the Caribbean Region. Theoretical and Applied Climatology, 86(1-4), 5-22. DOI 10.1007/s00704-005-0201-9.

Oleson, K., G. Niu, Z. Yang, D. Lawrence, P. Thornton, P. Lawrence, et al., 2008. "Improvements to the Community Land Model and Their Impact on the Hydrological Cycle." Journal of Geophysical Research 113: G01021. doi: http://dx.doi.org/10.1029/2007JG000563.

Oleson KW, Lawrence DM, Bonan GB et al (2013) Technical description of version 4.5 of the Community Land Model (CLM). NCAR technical note NCAR/TN-503 + STR. National Center for Atmospheric Research, Boulder

Paeth H. and Hense A., "SST versus climate change signals in West African rainfall: 20th-century variations and future projections," Climatic Change, vol. 65,no. 1-2, pp. 179–208, 2004.

Paeth H., Girmes R., Menz G., and Hense A., “Improving seasonal forecasting in the low latitudes,” Monthly Weather Review, vol. 134, no. 7, pp. 1859–1879, 2006.

Paeth H, Hall NM, Gaertner MA, Alonso MD, Moumouni S, Polcher J, Ruti PM, Fink AH, Gosset M, Lebel T, Gaye AT, Rowell DP, Moufouma-Okia W, Jacob D, Rockel B, Giorgi F, Rummukainen M. 2011. Progress in regional downscaling of West African precipitation. Atmos. Sci. Lett. 12(1): 75–82.

Pal JS, Small EE, Elthair EA (2000) Simulation of regionalscale water and energy budgets: representation of subgrid cloud and precipitation processes within RegCM. J Geophys Res 105: 29579–29594

Pal JS, Giorgi F, Bi X, Elguindi N, Solomon F, Gao X, Francisco R, Zakey A, Winter J, Ashfaq M, Syed F, Bell JL, Diffanbaugh NS, Kamacharya J, Konare A, Martinez D, da Rocha RP, Sloan LC, Steiner A (2007) The ICTP RegCM3 and RegCNET: regional climate modeling for the developing world. Bull Amer Meteor Soc 88:1395–1409

Reynolds RW, Smith TM (1994) Improved global sea surface temperature analysis using optimum interpolation. J Climate 7: 929–948

Simmons AS, Uppala DD, Kobayashi S (2007) ERA-interim: new ECMWF reanalysis products from 1989 onwards. ECMWF Newsl 110:29–35

Singh AP, Singh RP, Raju PVS, Bhatla R. 2011. Comparison of three different cumulus parameterization schemes on Indian summer monsoon circulation. Int. J. Ocean Clim. Syst. 2(1): 27–43

Smith SD (1988) Coefficients for sea surface wind stress, heat flux, and wind profiles as a function of wind speedand temperature. J Geophys Res 93: 15467–15472

Soden BJ, Held IM. 2006. An assessment of climate feedbacks in coupled ocean–atmosphere model. J. Clim. 19: 3354–3360.

Solmon F, Giorgi F, Liousse C (2006) Aerosol modeling for regional climate studies: application to anthropogenic particles and evaluation over a European/African domain. Tellus Ser B Chem Phys Meterol 58:51–72

Srinivas CV, Hariprasad D, Rao DVB, Anjaneyulu Y, Baskaran R, Venkataraman B. 2013. Simulation of the Indian summer monsoon regional climate using advanced research WRF model. Int. J. Climatol. 33: 1195–1210.

Steiner, A., J. Pal, S. Rauscher, J. Bell, N. Diffenbaugh, A. Boone, L. Sloan, et al.,2009. "Land Surface Coupling in Regional Climate Simulations of the West African Monsoon." Climate Dynamics 33: 869–892.

Sultan B, Janicot S. 2000. Abrupt shift of the ITCZ over West Africa and intra-seasonal variability. Geophysical Research Letters 27:3353–3356.

Sultan, B., Janicot, S., & Diedhiou, A. (2003). The West African monsoon dynamics. Part I: Documentation of intraseasonal variability. Journal of Climate, 16(21), 3389-3406.

Sultan B, Janicot S. 2003. The West African monsoon dynamics. Part II: The "preonset" and "onset" of the summer monsoon. J. Climate 16(21): 3407–3427.

Sundqvist HE, Berge E, Kristjansson JE (1989) The effects of domain choice on summer precipitation simulation and sensitivity in a regional climate model. J Climate 11: 2698–2712

Sylla MB, Gaye AT, Pal JS, Jenkins GS, Bi XQ. 2009. High resolution simulations of West Africa climate using Regional Climate Model (RegCM3) with different lateral boundary conditions. Theor. Appl. Climatol. 98(3–4): 293–314, DOI: 10.1007/s00704-009-0110-4.

Sylla MB, Giorgi F, Ruti PM, Calmanti S, Dell'Aquila A. 2011. The impact of deep convection on the West African summer monsoon climate: a regional climate model sensitivity study. Q. J. Roy. Meteorol. Soc. 137: 1417–1430, DOI: 10.1002/qj.853.

Sylla MB, Giorgi F, Stordal F. 2012. Large-scale origins of rainfall and temperature bias in high resolution simulations over Southern Africa. Climate Res. 52: 193–211, DOI: 10.3354/cr01044.

Sylla MB, Giorgi F, Coppola E, Mariotti L (2013a) Uncertainties in daily rainfall over Africa: assessment of observation products and evaluation of a regional climate model simulation. Int J Climatol. doi:10.1002/joc.3551

Sylla MB, Diallo I, Pal JS., 2013b. West African monsoon in state of the art regional climate models. In Climate Variability Regional and Thematic Patterns, Tarhule A (ed). ISBN: 980-953-307-816-3.

Tadross MA, Gutowski WJ Jr, Hewitson BC, Jack C, New M. 2006. MM5 simulations of interannual change and the diurnal cycle of
southern African regional climate. Theor. Appl. Climatol. 86(1–4): 63–80.

Thorncroft CD, Blackburn M (1999) Maintenance of the African easterly jet. Q J R Meteorol Soc 125:763–786

Tiedtke, M. 1989. “A Comprehensive Mass Flux Scheme for Cumulus Parameterization in Large-scale Models.” Monthly Weather Review 117: 1779–1800.

Uppala S, Dee D, Kobayashi S, Berrisford P, Simmons A (2008) Towards a climate data assimilation system: status update of ERA-interim. ECMWF Newsl 115:12–18

Wang, G., M. Yu, J. S. Pal, R. Mei, G. B. Bonan, S. Levis, and P. E. Thornton (2016), On the development of a coupled regional climate vegetation model RCM-CLM-CN-DV and its validation its tropical Africa, Clim. Dyn., 46, 515–539.

Xue Y, De Sales F, Lau KMW, Bonne A, Feng J, Dirmeyer P, Guo Z, Kim KM, Kitoh A, Kumar V, Poccard-Leclercq I, Mahowald N, Moufouma-Okia W, Pegion P, Rowell DP, Schemm J, Schulbert S, Sealy A, Thiaw WM, Vintzileos A, Williams SF, Wu ML (2010) Intercomparison of West African Monsoon and its variability in the West African Monsoon

Modelling Evaluation Project (WAMME) first model Intercomparison experiment. Clim Dyn. doi:10.1007/s00382-010-0778-2

Zakey AS, Solmon F, Giorgi F (2006) Implementation and testing of a desert dust module in a regional climate model. Atmos Chem Phys, 6:4687–4704

Zaroug MAH, Sylla MB, Giorgi F, Eltahir EAB, Aggarwal PK. 2012. A sensitivity study on the role of the Swamps of Southern Sudan in the summer climate of North Africa using a regional climate model. Theor. Appl. Climatol. DOI: 10.1007/s00704-012-0751-6.

Zeng X, Zhao M, Dickinson RE (1998) Intercomparison of bulk aerodynamic algorithms for the computation of sea surface fluxes using TOGA COARE and TAO DATA. J Climate 11: 2628–2644

	Guinea Coast		Central Sahel		West Sahel		West Africa	
	RMSE (°C)	PCC	RMSE (°C)	PCC	RMSE (°C)	PCC	RMSE (°C)	PCC
UDEL	0.613	0.749	0.475	0.974	0.424	0.981	0.695	0.981
Mix1	1.605	0.768	0.737	0.961	0.720	0.987	1.218	0.978
Emanuel	1.294	0.772	0.673	0.954	0.589	0.986	1.068	0.979
Grell	2.657	0.728	1.406	0.920	1.994	0.985	2.171	0.973
Tiedtke	1.534	0.758	1.360	0.938	0.717	0.982	1.355	0.938
Mix2	1.993	0.781	1.682	0.884	1.568	0.978	1.715	0.964

Table 1: Pattern correlation coefficient (PCC) and root mean square difference (RMSD) for JJAS 2m-temperature for model simulations and observation (UDEL) with respect to CRU over sub-regions Guinea Coast, Central Sahel, West Sahel and West Africa domain during the period 2002-2003.

	Guinea Coast	Central Sahel	West Sahel	West Africa	
	Mean Bias (%)	Mean Bias (%)	Mean Bias (%)	Mean Bias (%)	PCC
TRMM	5	-5.11	4.26	1.24	0.963
Mix1	-18.49	-40.15	-15.07	-22.25	0.719
Emanuel	-27.92	-42.71	-33.56	-25.58	0.807
Grell	-44.29	-56.62	-51.74	-34.07	0.641
Tiedtke	-53.54	-77.14	-56.69	-65.08	0.609
Mix2	-53.44	-50.67	-55.76	-47.66	0.893

Table 2: Mean bias (MB) and the pattern correlation coefficient (PCC) for JJAS precipitation for model simulations and observation (TRMM) with respect to GPCP for sub-regions Guinea Coast, Central Sahel, West Sahel and West Africa domain. The PCC is calculated only for the West African domain during the period 2002-2003.

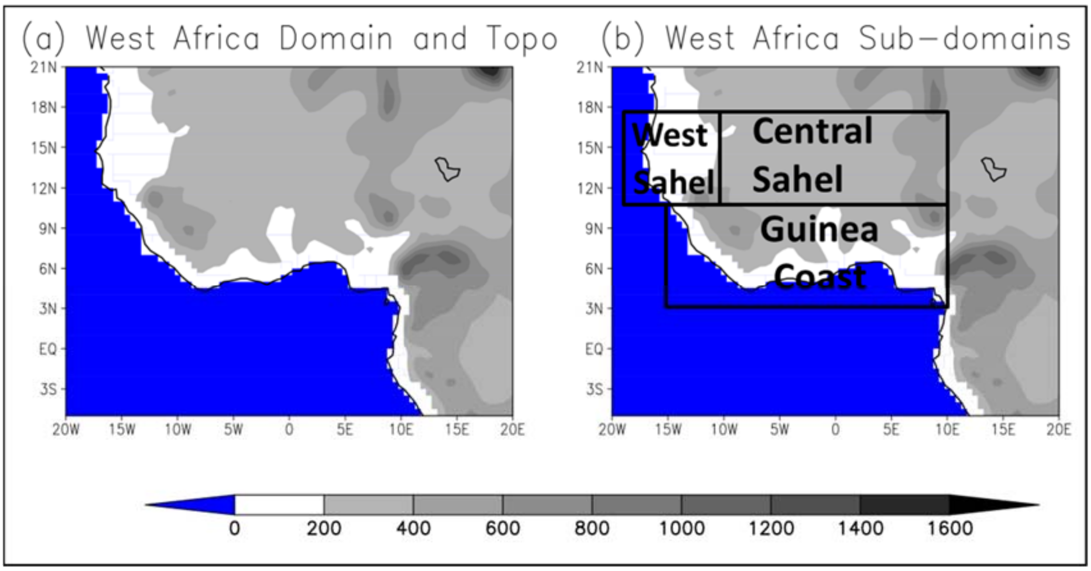

Figure 1: Topography of the West African domain. The analysis of model result is emphasis over the whole West African domain and the three sub-regions Guinea Coast, Central Sahel and West Sahel which are marked with black boxes.

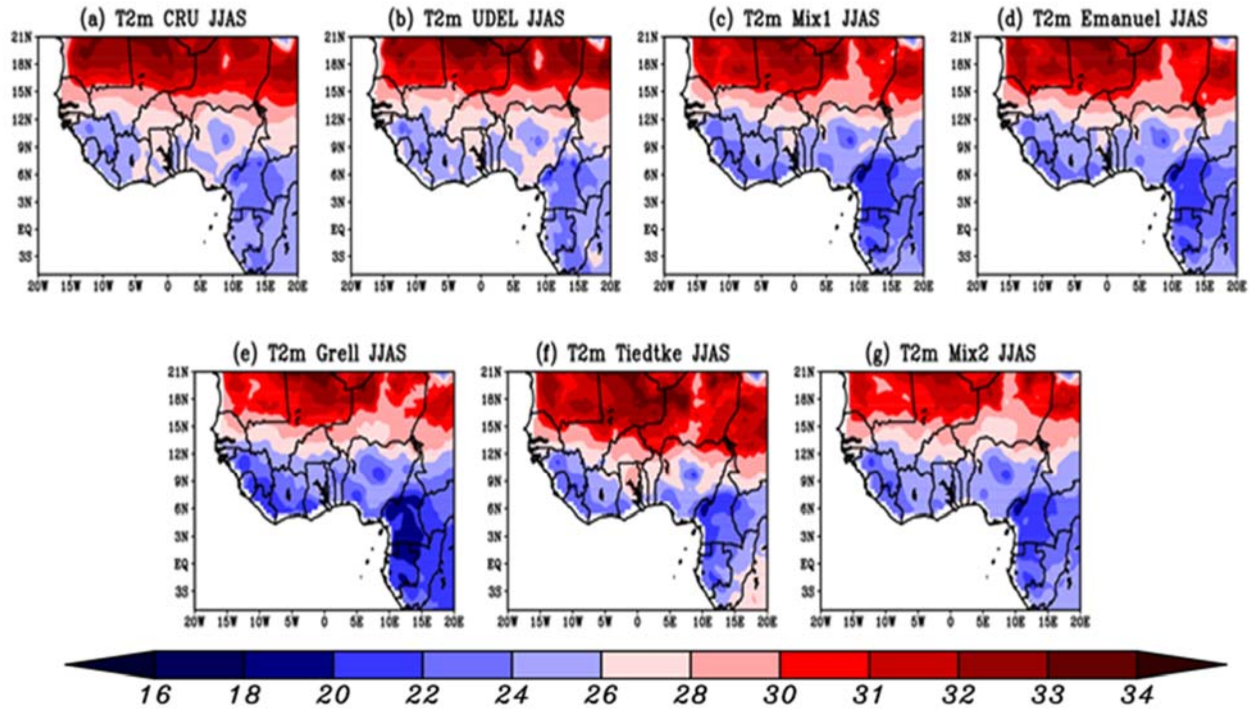

Figure 2: Averaged 2003–2004 JJAS 2m-temperature (in °C) over West Africa from: (a) CRU, (b) UDEL, (c) Mix1, (d) Emanuel, (e) Grell, (f) Tiedtke and (g) Mix2.

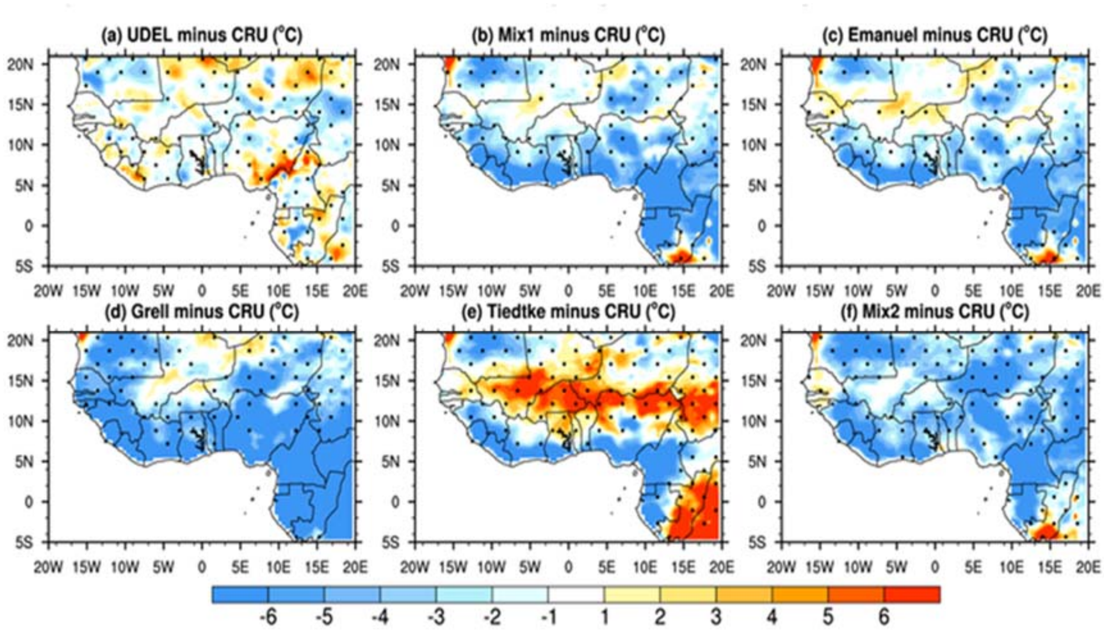

Figure 3: JJAS 2m-temperature bias (in °C), over West Africa, with respect to CRU from: (a) UDEL, (b) Mix1, (c) Emanuel, (d) Grell, (e) Tiedtke and (f) Mix2 during the period 2002-2003. The dotted area denotes differences which are statistically significant at a significance level of 0.05.

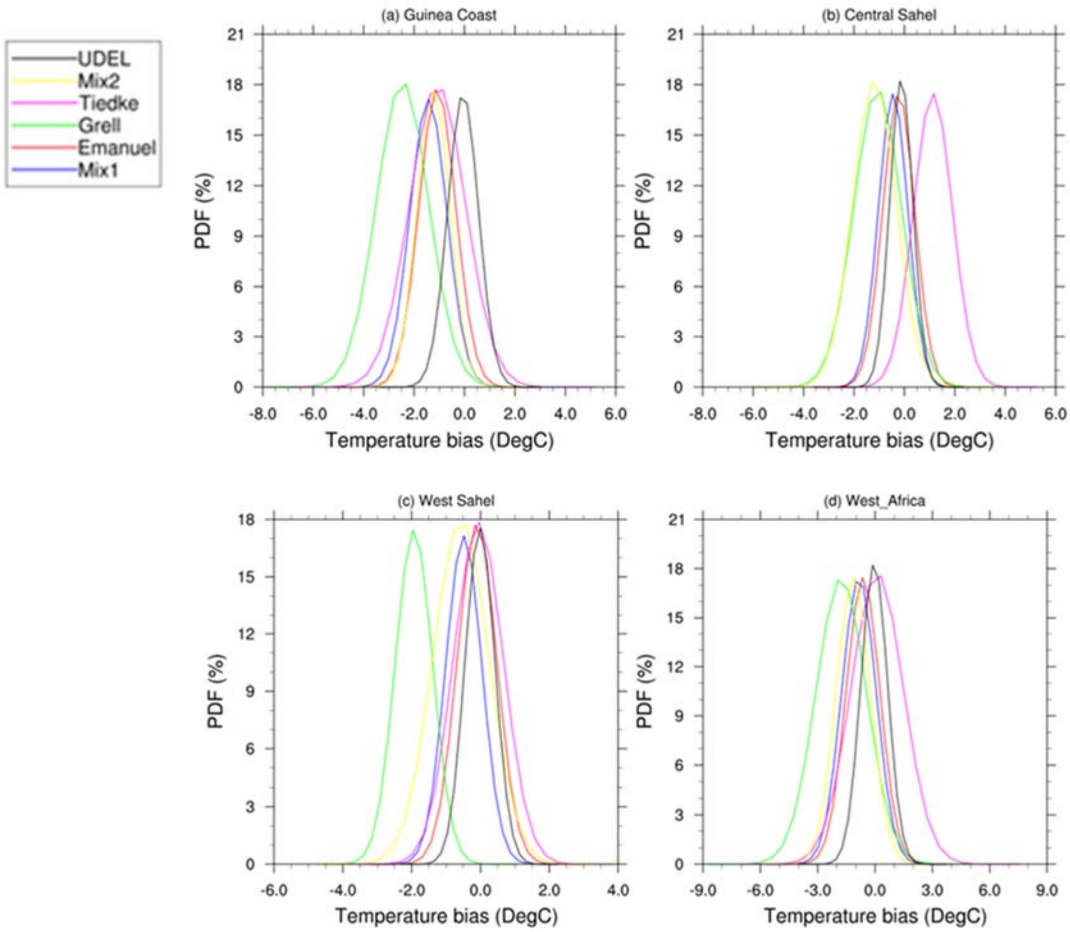

Figure 4: PDF distributions (%) of temperature bias in JJAS over Guinea, Central Sahel, West Sahel and West Africa, derived from the model simulations using different convection schemes (land only; units: °C) during the period 2002-2003.

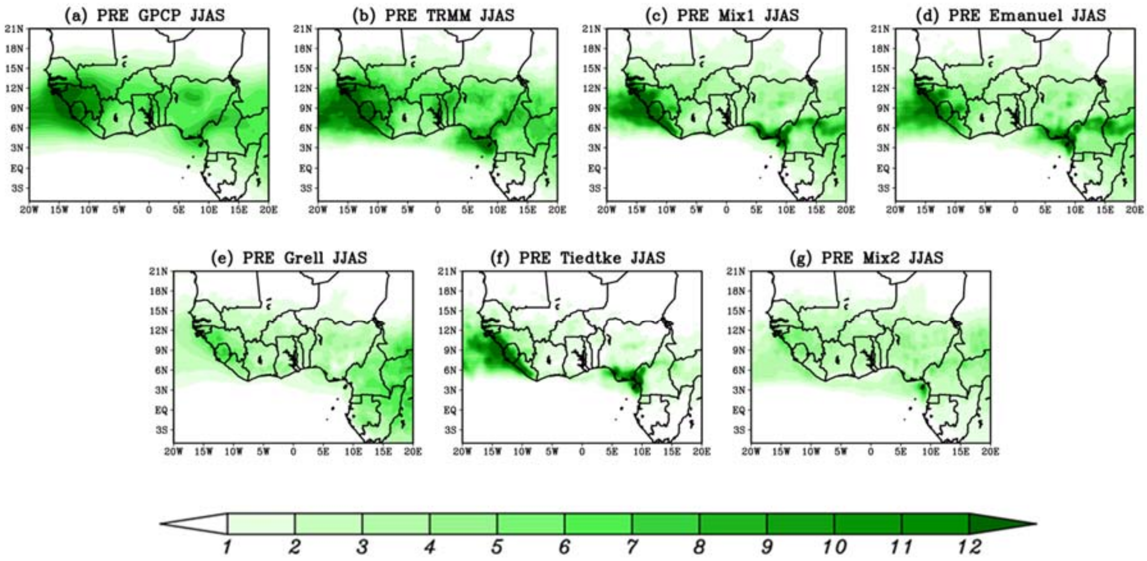

Figure 5: Averaged 2003–2004 JJAS precipitation (in mm/day) over West Africa from: (a) GPCP, (b) TRMM, (c) Mix1, (d) Emanuel, (e) Grell, (f) Tiedtke and (g) Mix2.

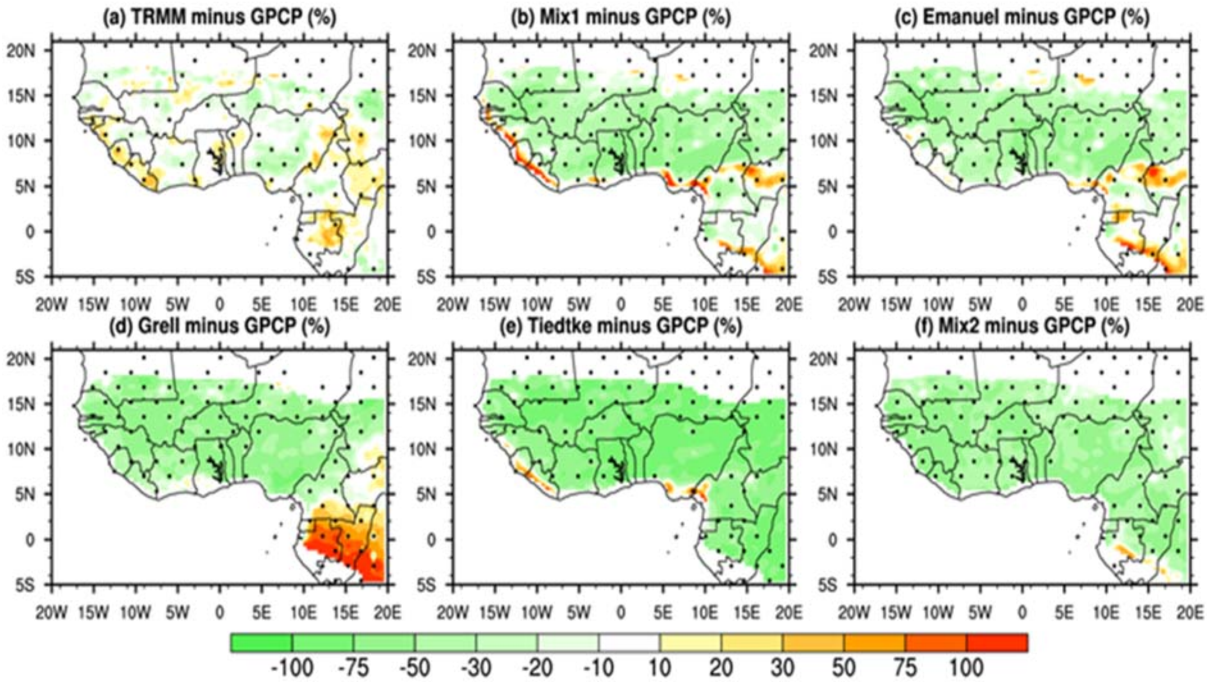

Figure 6: JJAS precipitation bias (in %), over West Africa, with respect to GPCP from : (a) TRMM, (b) Mix1, (c) Emanuel, (d) Grell, (e) Tiedtke and (f) Mix2 during the period 2002-2003.

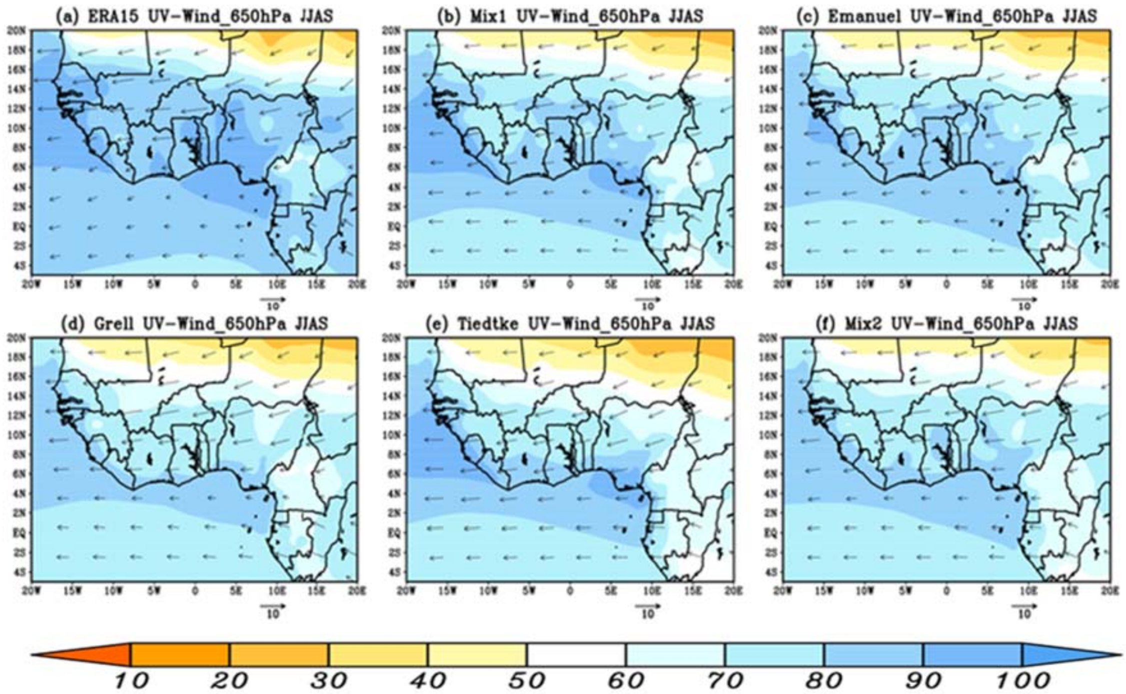

Figure 7: The (a) observed and (b–f) simulated vertically mean midlevel (850–300 hPa) integrated specific humidity (shaded) superimposed at zonal winds in JJAS at 650 hPa, over West Africa, from: (a) ERA-Interim, (b) Mix1 (c) Emanuel, (d) Grell (e) Tiedtke and (f) Mix2. Arrows are in m/s and specific humidity is expressed in 10^{-3} kg/kg during the period 2002-2003.

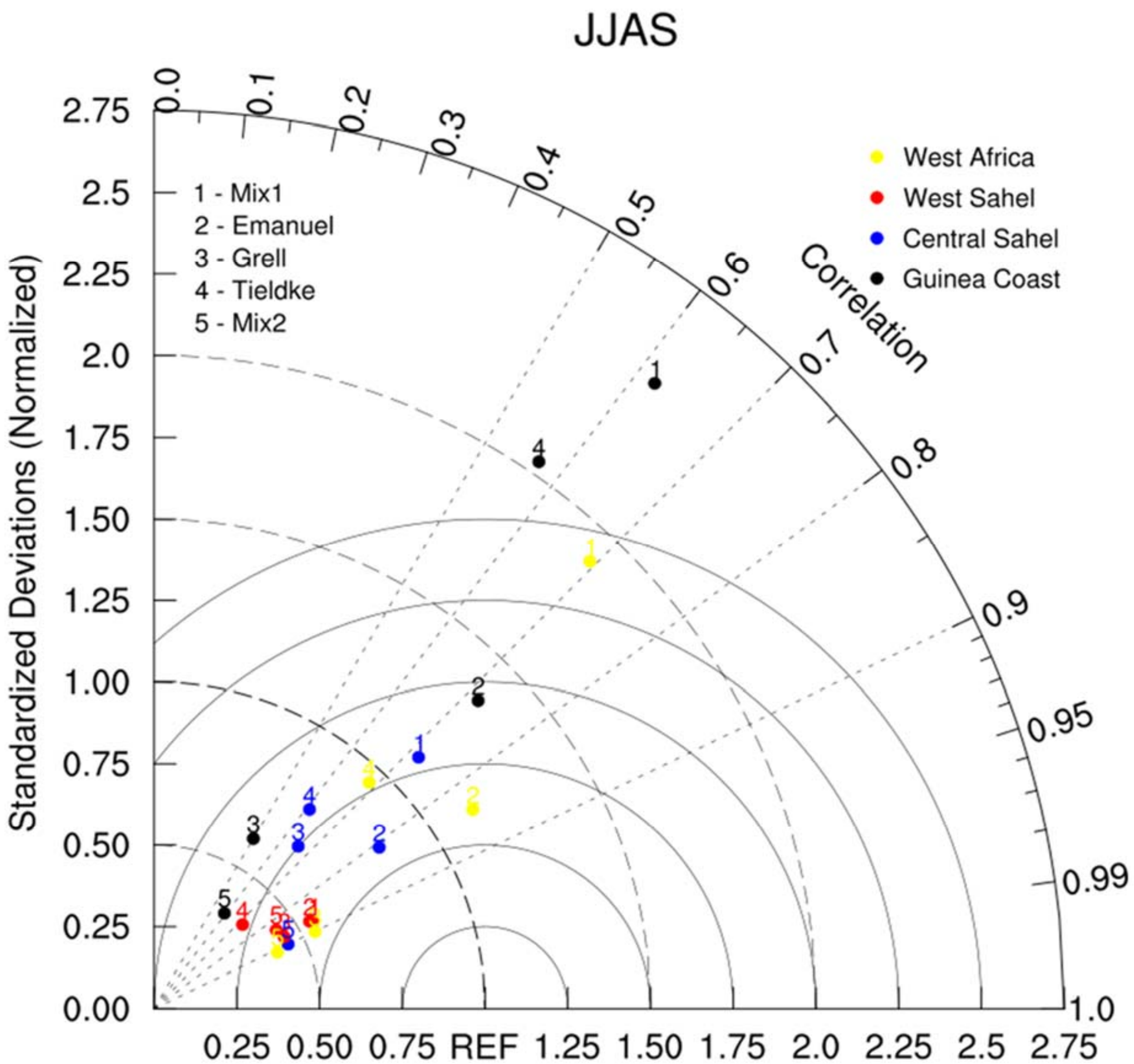

Figure 8: Taylor diagram showing the pattern correlation and the standard deviation (Normalized) for JJAS precipitation with respect to GPCP from: Mix1, Emanuel, Grell, Tiedtke and Mix2 over Guinea Coast, Central Sahel, West Sahel and West Africa during the period 2002-2003**.**

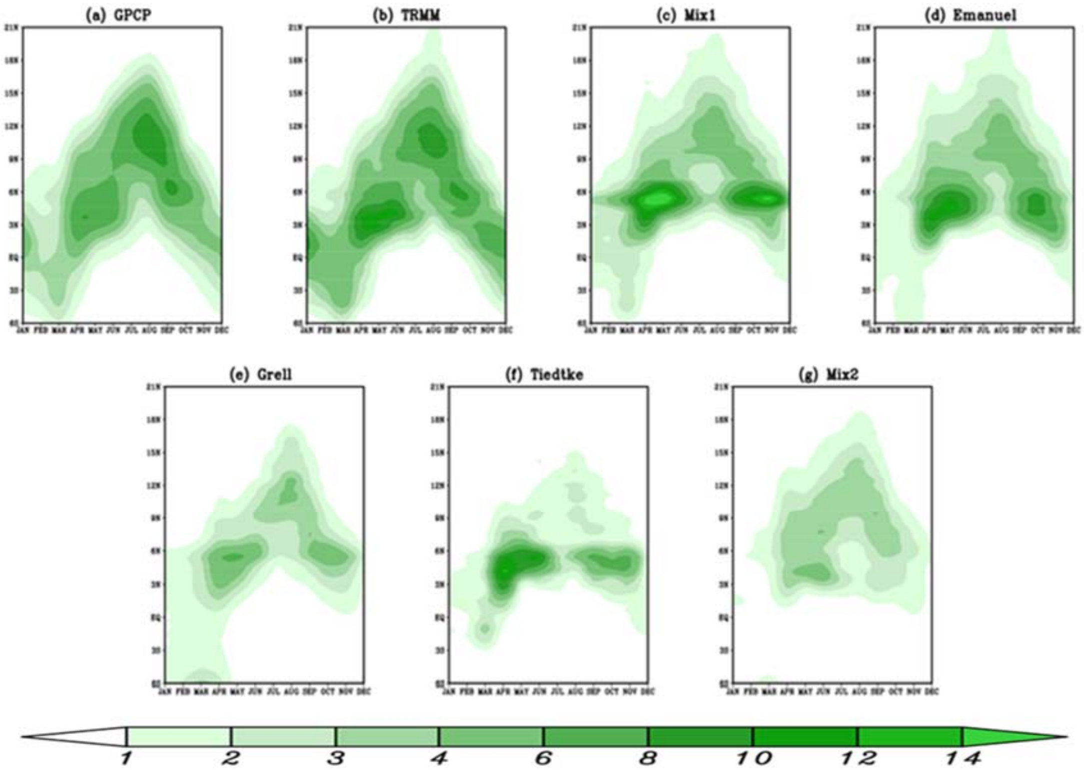

Figure 9: Hovmoller diagram of monthly precipitation (mm/day) averaged between 10°W and 10°E and for the period 2003-2004 for (a) GPCP, (b) TRMM, (c) Mix1, (d) Emanuel, (e) Grell, (f) Tiedtke and (g) Mix2 under different convective schemes: Mix1, Emanuel, Grell, Tiedke and Mix2.

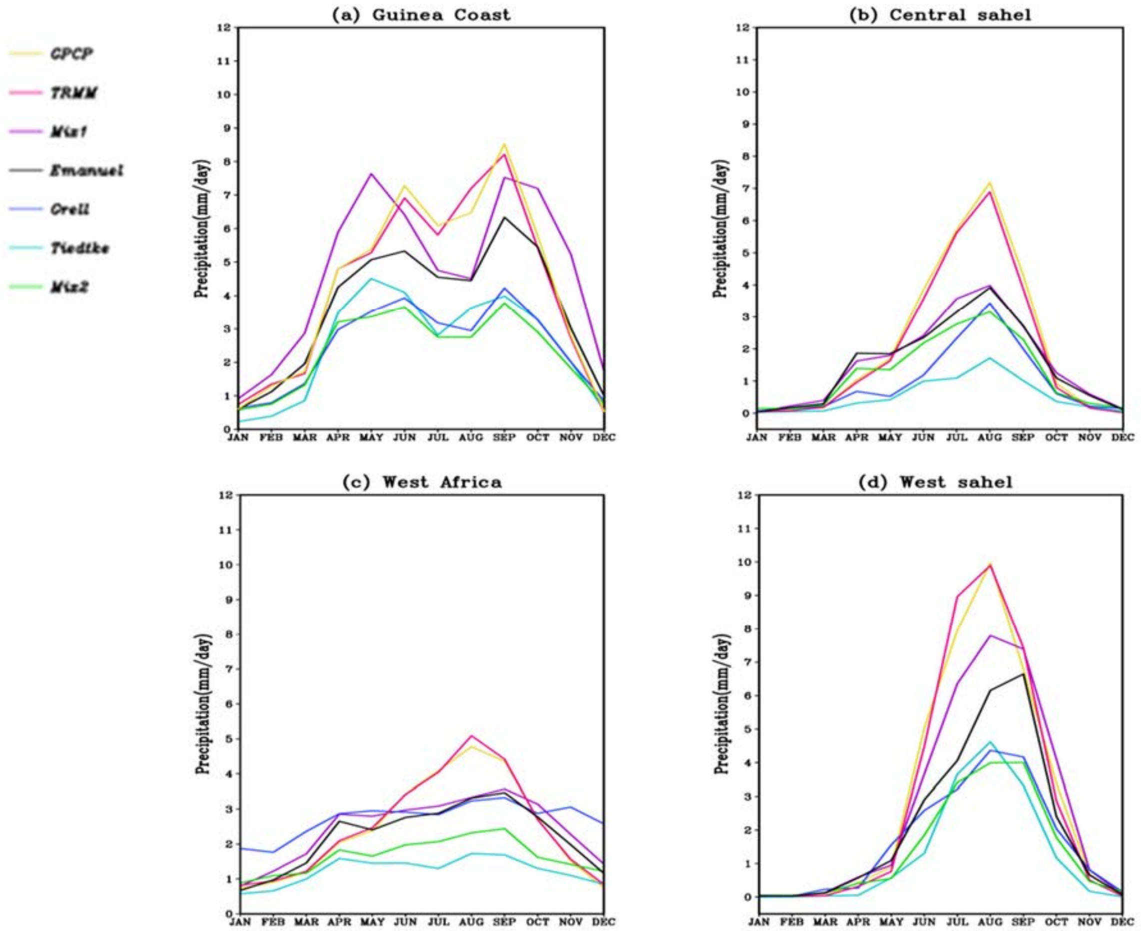

Figure 10: Annual cycle of monthly precipitation (mm.day^{-1}) averaged over, (a) the Guinea Coast West and (b) Central Sahel, (c) West Africa and (d) West Sahel for the period 2003–2004 under different convective schemes: Mix1, Emanuel, Grell, Tiedke and Mix2.

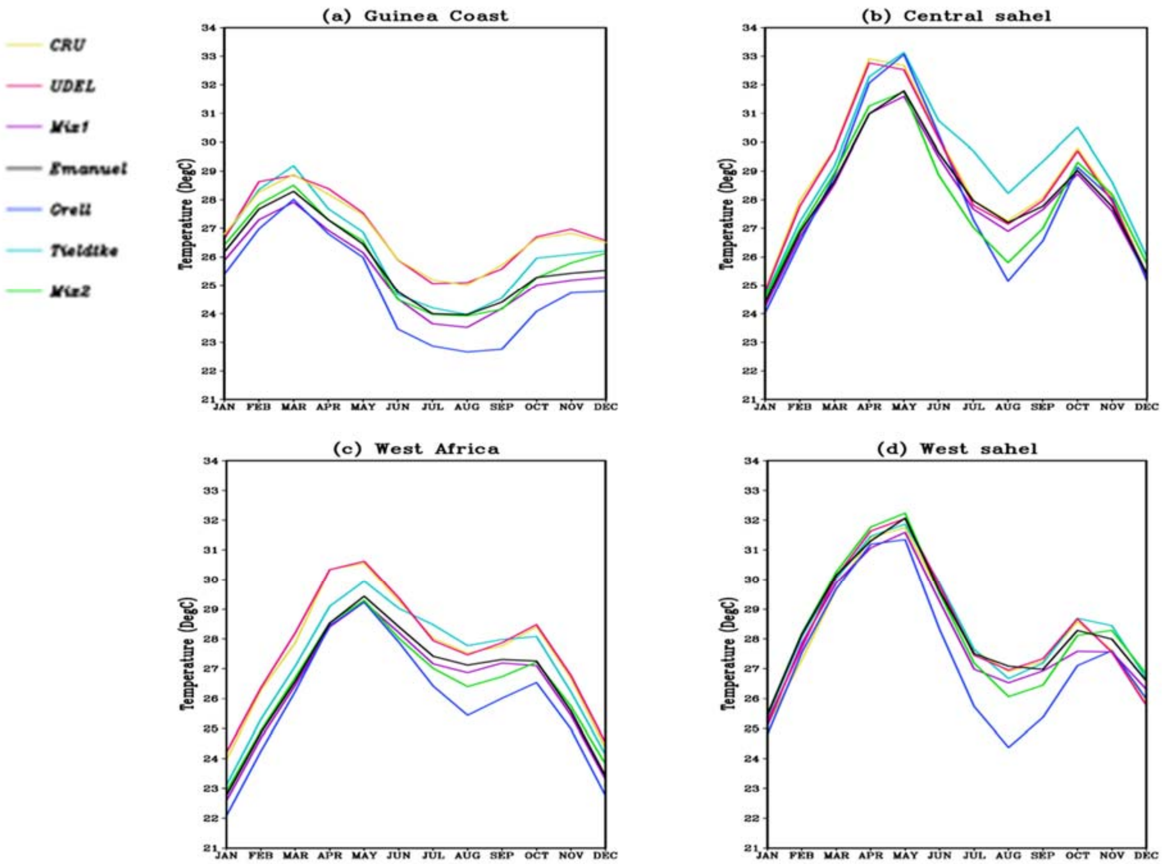

Figure 11: Annual cycle of 2m-Temperature (°C) averaged over, (a) the Guinea Coast, (b) Central Sahel, (c) West Africa and (d) West Sahel for the period 2003–2004 under different convective schemes: Mix1, Emanuel, Grell, Tiedke and Mix2.

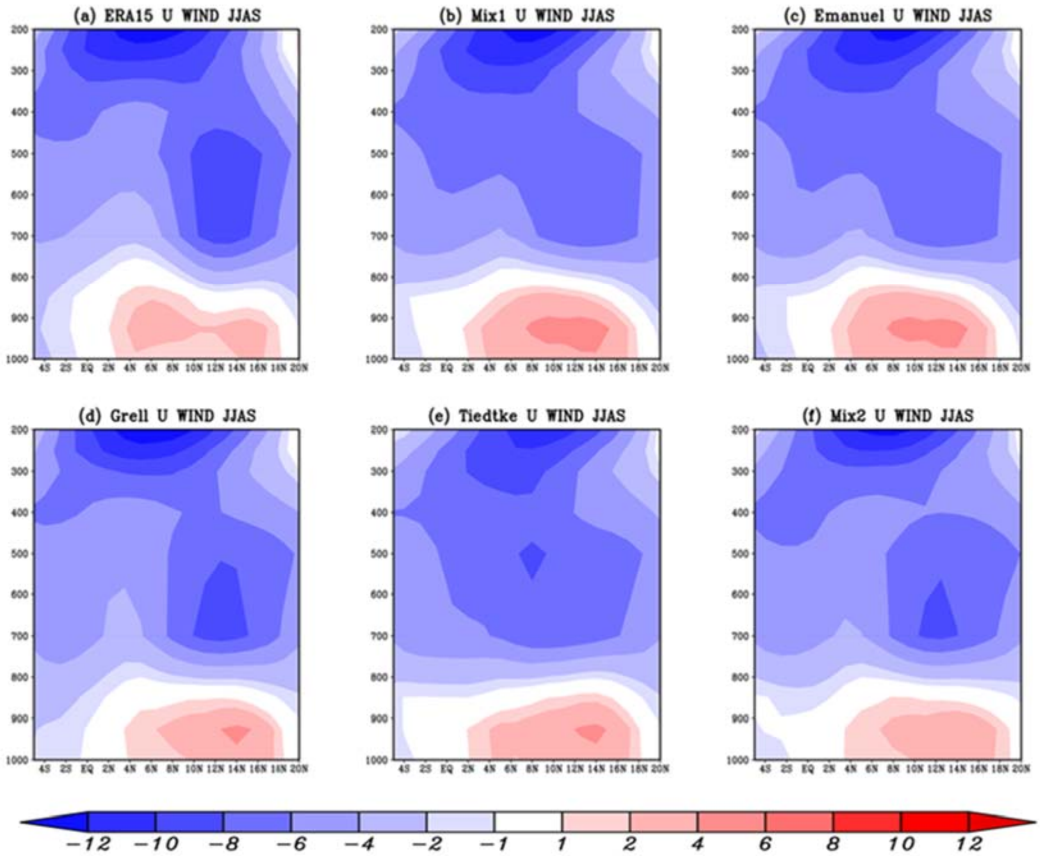

Figure 12: Vertical cross section of the JJAS mean zonal wind (in m/s) averaged between 10°W–10°E, over West Africa, from: (a) ERA-Interim (b) Mix1, (c) Emanuel, (d) Grell, (e) Tiedtke and (f) Mix2. The mean is calculated using the 2003–2004 period.